

# Ubiquitous Strategy for Probing ATR Surface-Enhanced Infrared Absorption at Platinum Group Metal–Electrolyte Interfaces

Yan-Gang Yan,<sup>†</sup> Qiao-Xia Li,<sup>†</sup> Sheng-Juan Huo,<sup>†</sup> Min Ma,<sup>†</sup> Wen-Bin Cai,<sup>\*,†</sup> and Masatoshi Osawa<sup>‡</sup>

Shanghai Key Laboratory for Molecular Catalysis and Innovative Materials and Department of Chemistry, Fudan University, Shanghai 200433, China, and Catalysis Research Center, Hokkaido University, Sapporo 001-0021, Japan

Received: December 29, 2004; In Final Form: February 24, 2005

A versatile two-step wet process to fabricate Pt, Pd, Rh, and Ru nanoparticle films (simplified as nanofilms hereafter) for in situ attenuated total reflection Fourier transform infrared (ATR-FTIR) study of electrochemical interfaces is presented, which incorporates an initial chemical deposition of a gold nanofilm on the basal plane of a silicon prism with the subsequent electrodeposition of desired platinum group metal overlayers. Galvanostatic electrodeposition of Pt, Rh, and Pd from phosphate or perchloric acid electrolytes, or potentiostatic electrodeposition of Ru from a sulfuric acid electrolyte, yields sufficiently “pinhole-free” overlayers as evidenced by electrochemical and spectroscopic characterizations. The Pt group metal nanofilms thus obtained exhibit strongly enhanced IR absorption. In contrast to the corresponding metal films electrochemically deposited directly on glassy carbon and bulk metal electrodes, the observed enhanced absorption for the probe molecule CO exhibits normal unipolar band shapes. Scanning tunneling microscopic (STM) images reveal that fine nanoparticles of Pt group metals are deposited around wavy and stepped bunches of Au nanoparticles of relatively large sizes. This ubiquitous strategy is expected to open a wide avenue for extending ATR surface-enhanced IR absorption spectroscopy to explore molecular adsorption and reactions on technologically important transition metals, as exemplified by successful real-time spectroscopic and electrochemical monitoring of the oxidation of CO at Pd and that of methanol at Pt nanofilm electrodes. The spectral features of free water molecules coadsorbed with CO on Pt, Pd, Rh, and Ru are also discussed.

## Introduction

Surface-enhanced infrared absorption spectroscopy (SEIRAS) has received increasing attention in surface science and electrochemistry because of its high signal sensitivity and a simple surface selection rule.<sup>1–10</sup> Although external IR reflection absorption spectroscopy (IRAS) has been widely used in these fields, it has several inherent problems in application to electrochemistry, such as high solution resistance, inhomogeneous current distribution, and limited mass transport, which are caused by pressing the working electrode against a cell window to reduce the strong absorption by the electrolyte solution.<sup>11</sup> SEIRAS in an attenuated-total-reflection (ATR) mode, ATR-SEIRAS, is free from these problems and has been applied successfully to the real-time monitoring of adsorption and reactions at electrode surfaces.<sup>9,10,12</sup>

A key issue for successfully implementing this technique is the fabrication of nanoparticle metal films with well-tuned size, shape, and proximity so that a strong SEIRA effect can be obtained. For in situ surface electrochemistry application, additional requirements for these nanofilms to serve as qualified electrodes are conductivity and stability in solution. There are generally two strategies for fabricating the nanofilms for in situ electrochemical SEIRA spectroscopy. The first one is referred to dry processes, involving vacuum evaporation and sputtering;

the second one is referred to wet processes, consisting of electrochemical and electroless (i.e., chemical) depositions.

Although dry processes have predominantly been used in depositing various metals and alloys, including Au, Ag, Pt, and Ru as well as Pt–Fe and Pt–Ru alloy nanofilms on IR windows as working electrodes in earlier ATR-SEIRAS measurements,<sup>1–8,12,13</sup> several disadvantages exist such as the requirement of a high-cost vacuum evaporator, time-consuming operation, poor enhancement reproducibility, and sample contamination by organic species. What is more, the emergence of severely distorted bipolar IR absorption bands seen frequently for vacuum-deposited transition metals such as Pt, Ru, and Pt alloy films complicates the analysis and explanation of spectral data.<sup>8,12,13</sup>

Electrodeposition is a wet process applicable to the deposition of many metals and has been used for external reflection SEIRAS measurements on Pt group metals.<sup>14–17</sup> Nevertheless, many reported enhanced spectra therein are severely distorted as in the case of dry processes. Specifically for Pt group metals electrochemically deposited on a glassy carbon electrode, the enhanced IR bands are observed with negative absorption and tremendously broadened bandwidth. These spectral features were named as abnormal infrared effects (AIREs) by Sun’s group.<sup>15</sup> The origin of the distorted band shapes is believed to be specific morphologies of the deposited metals (shape, size, and proximity of the metal particles).<sup>14,18</sup> It should also be noted that the electrodeposition technique is not suitable for ATR-SEIRAS measurements because nondoped (i.e., nonconductive) Si prisms

\* Corresponding author. Phone: +86-21-55664050. Fax: +86-21-65641740. E-mail: wbcai@fudan.edu.cn.

<sup>†</sup> Fudan University.

<sup>‡</sup> Hokkaido University.

are generally used in the measurements due to high chemical stability and high transmittance.

Very recently, electroless deposition, an alternative wet process, has been introduced to make SEIRA-active Au, Pt, Ag, and Cu nanofilms on Si and Ge windows.<sup>9,10,18,19</sup> This simple wet process can overcome the disadvantages of the dry processes and yield a stronger SEIRA effect. In addition, the chemically deposited metal films are more stable in solutions than vacuum-evaporated ones.<sup>9,10,18,19</sup> Unfortunately, so far the success of the electroless deposition method (tentatively called the one-step wet process) has been restricted to Au, Pt, Ag, and Cu. In addition, a patented commercial electrolyte with unknown additives was used to produce Pt nanofilms.<sup>9</sup>

The main purpose of the current work is to develop a ubiquitous two-step wet-process strategy for in situ electrochemical ATR-SEIRAS application. This strategy incorporates the electroless deposition of an SEIRA-active Au nanofilm on Si with subsequent electrodeposition of a desired metal overlayer. Similar tactics have been utilized by Weaver's group to obtain surface-enhanced Raman scattering (SERS) on Pt, Pd, Rh, and Ir surfaces that show in nature far weaker SERS activity than Ag, Au, and Cu surfaces.<sup>20,21</sup> In their work, a Au bulk surface was initially roughened by an oxidation–reduction cycle (ORC) pretreatment in KCl to yield SERS effect and then was covered by electrodeposition of an ultrathin overlayer of a Pt group metal. With selected deposition conditions, they obtained virtually pinhole-free SERS-active Pt, Pd, Rh, and Ir surfaces. The basic idea of the SERS experiment is the use of the SERS activity of the underlying Au surface to probe the surface of the overlayer. Since SERS is a relatively short-ranged effect, the thickness of the overlayers should be confined to a few monolayers. Therefore, the preparation of pinhole-free overlayers is not easy. The basic idea of the two-step wet process for ATR-SEIRAS proposed here is slightly different and 2-fold. First is the extension of metals available for ATR-SEIRAS by using an electrochemical deposition technique. By using a conducting Au underlayer, electrodeposition becomes possible. Second is to solve the band distortion problem by using an SEIRA-active Au film as a template. Different from SERS, a significant SEIRA effect is not limited to coinage metals,<sup>2</sup> and thus thicker transition metal overlayers can be used, which facilitates the preparation of pinhole-free overlayers. We will demonstrate herein the feasibility of our two-step wet process by applying it to Pt group metals (including Pt, Pd, Rh, and Ru). The electrochemical and IR results reveal that sufficiently pinhole-free Pt, Rh, Pd, and Ru overlayers that exhibit significant SEIRA effects and normal electrochemical properties can be prepared by this simple method.

## Experimental Section

**Nanofilm Preparation.** A hemicylindrical Si prism was polished and then cleaned with the RCA method:<sup>22</sup> i.e., soaking it in a 1:1:5 (v/v) solution of NH<sub>3</sub>, H<sub>2</sub>O<sub>2</sub>, and H<sub>2</sub>O, and afterward in a 1:1:5 (v/v) solution of HCl, H<sub>2</sub>O<sub>2</sub>, and H<sub>2</sub>O at about 80 °C, followed by thorough rinsing with water. Then the total-reflecting plane was immersed in 40% NH<sub>4</sub>F solution for 1.5 min to terminate the Si surface with hydrogen. The chemical deposition of a Au film on Si was performed according to the procedures and recipes reported by Miyake et al.<sup>19</sup>

The electrodeposition of Pt, Pd, Rh, and Ru overlayers was carried out in selected plating electrolytes with the Au film, a saturated calomel electrode (SCE), and a Pt mesh serving as the working (working area 1.54 cm<sup>2</sup>), reference, and counter electrodes, respectively. Galvanostatic mode was employed for

the deposition of Pt, Rh, and Pd overlayers according to the recipes reported by Zou et al.<sup>20</sup> Briefly, the plating solution consists of 4 mM H<sub>2</sub>PtCl<sub>6</sub>·6H<sub>2</sub>O and 0.7 M Na<sub>2</sub>HPO<sub>4</sub> for Pt overlayer, 5 mM PdCl<sub>2</sub> and 0.1 M HClO<sub>4</sub> for Pd, and 5 mM RhCl<sub>3</sub>·5H<sub>2</sub>O and 0.1 M HClO<sub>4</sub> for Rh. Pd was electrodeposited at 20 μA for 180 s, Rh at 100 μA for 100 s, and Pt at 400 μA for 160 s. Potentiostatic mode was used for the deposition of Ru multilayers as suggested by Strbac et al.<sup>23</sup> Ru overlayer was electrodeposited onto Au at −0.25 V for 600 s and then at −0.2 V for 900 s in a plating electrolyte containing 0.1 mM RuCl<sub>3</sub> and 0.5 M H<sub>2</sub>SO<sub>4</sub>.

Inductively coupled plasma (ICP) atomic emission spectroscopy (AES) was used to determine the concentrations of dissolved metallic ions from the metal films (Au, Pt, Pd, and Ru) on Si in hot aqua regia. With known masses of the deposits, the average thicknesses of the deposits were estimated by assuming the same densities as their bulk materials. For the Rh nanofilm, the cathodic charge accumulated during electrodeposition was used to estimate its average thickness.<sup>20</sup> The thicknesses of Au, Pd, Pt, Rh, and Ru nanofilms were around 65, 1.4, 6.1, 2.4, and 4.6 nm, respectively, by taking the geometric area for working electrodes. The existence of pinholes in the overlayers was examined by voltammetry and SEIRAS using CO as a probe molecule.

**SEIRA Spectroscopy, Electrochemistry, and Scanning Tunneling Microscopy (STM).** A Nicolet Magna-IR 760 FTIR spectrometer equipped with a liquid nitrogen cooled HgCdTe MCT detector was used for SEIRAS measurements and was operated at a resolution of 4 (for potentiostatic multistep measurements) or 8 cm<sup>−1</sup> (for potentiodynamic kinetics measurements). Spectra of the Pt group metal/solution interfaces were acquired with the so-called Kretschmann attenuated-total-reflection (ATR) configuration (prism/thin metal film/solution geometry), details of which can be found elsewhere.<sup>2,24</sup> Unpolarized infrared radiation from a ceramic source was focused at the interface by being passed through the prism at the incident angle of 70°, and the totally reflected radiation was detected. Spectra were acquired under potentiostatic or potentiodynamic conditions. All the spectra in this paper are shown in the absorbance units defined as  $-\log(I/I_0)$ , where  $I$  and  $I_0$  represent the intensities of the reflected radiation at the sample and reference potentials, respectively. The adsorption and oxidation of CO on the above-mentioned four nanofilms and the oxidation of methanol on a Pt nanofilm were taken as the prototype electrocatalytic reactions to check the validity of our strategy in electrochemical ATR-SEIRAS.

A CHI 630B electrochemistry workstation was employed for potential/current control and to record the cyclic voltammograms. All electrode potentials are cited with a reversible hydrogen electrode (RHE), unless specifically addressed.

Ex situ STM observation of the nanofilms was carried out with a Molecular Imaging Pico-SPM. Tunneling tips were prepared by electrochemical etching of a tungsten wire (0.25 mm in diameter). All STM images shown in this paper were acquired in the constant-current mode with  $V_b = 0.1$  V and  $I_t = 5$  nA.

## Results and Discussion

**Electrochemical Properties.** Cyclic or linear sweep voltammetry was used to evaluate the electrochemical properties of deposited overlayers. Voltammograms of electrodeposited Pd, Pt, and Rh overlayers on Au/Si in 0.1 M HClO<sub>4</sub> and CO-saturated 0.1 M HClO<sub>4</sub> at 50 mV s<sup>−1</sup> are shown in Figure 1A–C (A, Pd; B, Pt; C, Rh). Dashed traces 1 in Figure 1A–C show

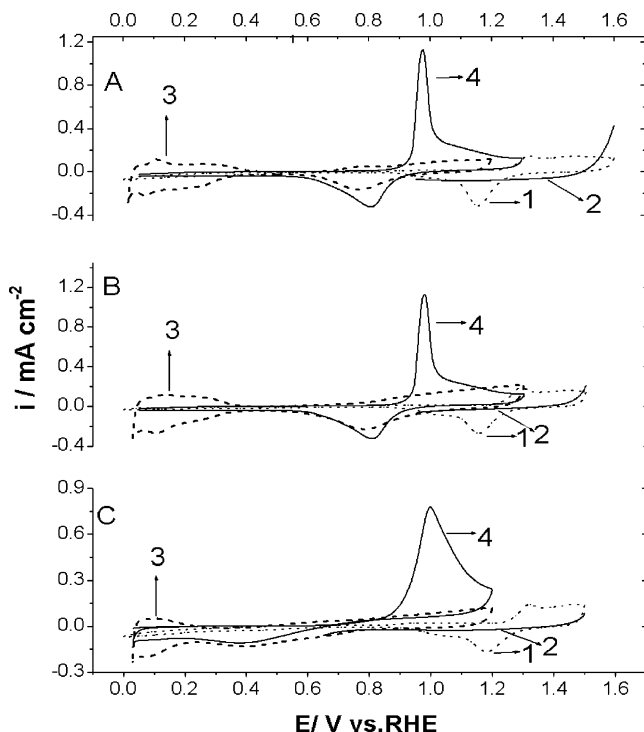


**Figure 1.** Cyclic voltammograms of Pd (A), Pt (B), and Rh (C) coated Au nanofilm electrodes in 0.1 M HClO<sub>4</sub> in the absence (traces 3) and presence (traces 4) of saturated CO. Traces 1 represent cyclic voltammograms for bare Au nanofilm electrodes, and traces 2 represent linear voltammograms of Pd, Pt, or Rh coated Au nanofilms in 0.1 M HClO<sub>4</sub> recorded after holding the potential at 1.5–1.6 V for 5 s. Scan rate: 50 mV s<sup>-1</sup>.

cyclic voltammograms of unmodified Au films before depositing overlayers of Pd, Pt, and Rh, respectively. The typical voltammetric features of polycrystalline Au can be found with the onset of anodic oxide formation at high potentials (>1.3 V) and its reduction peak at 1.15 V in the backward half-cycle. Trace 2 in Figure 1A represents the voltammogram of a Pd-coated Au film for a linear potential sweep from 1.6 to 0.9 V after holding the electrode potential at the positive limit for 5 s. This potential range is high enough for Au oxidation, but the cathodic peak corresponding to the reduction of Au oxide is entirely absent, indicating that the Pd overlayer covers essentially the entire gold surface, at least to block the Au oxide formation. Constant-current deposition of 1.4-nm-thick Pd overlayer was sufficient to remove the Au oxide features and replace them with voltammetric characteristics similar to those for a polycrystalline Pd bulk electrode. Similar results were obtained for Pt (Figure 1B) and Rh (Figure 1C) overlayers formed by galvanostatic deposition, although thicker ones were needed for the Pt and Rh to achieve the sufficiently pinhole-free property. The charges of hydrogen adsorption obtained for Pd, Pt, and Rh are 623, 513, and 400  $\mu\text{C cm}^{-2}$ , respectively.

Since oxygen evolution is significant on Ru even at lower potentials, the linear sweep voltammetric evaluation was not applied for Ru-coated electrodes to avoid being damaged by rigorous oxygen evolution. The resultant voltammograms are close to those of a bulk polycrystalline Ru electrode reported by Gutierrez et al.<sup>25</sup> The irreversible redox behavior of the Ru-coated electrode prevents the evaluation of the charge for hydrogen adsorption. To solve this problem, cyclic voltammetry was carried out in 0.1 M NaOH instead of the acidic solution, the result for which is shown in Figure 2 (lower panel). The peaks at 0–0.2 V have been attributed to hydrogen adsorption and desorption.<sup>25</sup> By integrating the peaks, a hydrogen adsorp-

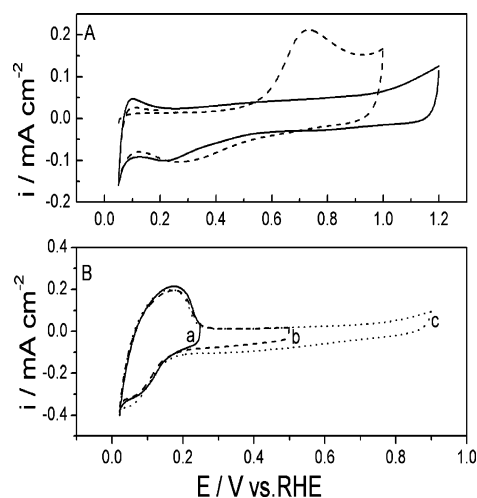


**Figure 2.** Cyclic voltammograms of Ru-coated Au nanofilm electrode in 0.1 M HClO<sub>4</sub> in the absence (solid line) and presence (dashed line) of saturated CO (A), and in 0.1 M NaOH with varying positive limits (B). Scan rate: 50 mV s<sup>-1</sup>.

tion charge of around 559  $\mu\text{C cm}^{-2}$  can be estimated for the electrodeposited Ru overlayer.

Assuming 210  $\mu\text{C cm}^{-2}$  for the hydrogen adsorption charge at an ideal smooth electrode, the roughness factors are within 2–3 for the deposited Pd, Pt, Rh, and Ru overlayers, which are slightly larger than polished bulk electrodes used in external IRAS measurement (typically 1.5–2).

The structures of the thin films prepared by electrodeposition were characterized using ex situ scanning tunneling microscopy. The images of a bare Au film and Pt group metal coated Au films are shown in Figure 3. The bare Au film consists of cascading slatellike crystallites, showing a face-centered-cubic structure. The morphology of the Au film was totally changed after the electrodeposition of Pd, Pt, Rh, and Ru. Basically, rather small and compact irregular island crystallites of Pt, Pd, Rh, and Ru grow on the Au film substrates with particle sizes and substructures varying with metallic elements. It is noted that the nanofilms thus obtained are quite different in particle shapes from the corresponding ones formed by cyclic voltammetric deposition on a glassy carbon.<sup>15</sup> In the latter, the nanostructures with stacked layers were formed and the films show an antiabsorption band feature (i.e., one of AIREs). The specific nanostructures may be a possible origin of the antiabsorption band feature.

**SEIRA Spectra of Adsorbed CO.** To check further whether the Au surface was sufficiently covered by the electrodeposited overlayers, CO was used as the probe molecule since the C–O stretching mode is sensitive to the adsorption sites. Previous ATR-SEIRAS results<sup>19,26</sup> indicate that CO adlayer on a bare Au film on Si exhibits a major band ranging from 2110 to 2135  $\text{cm}^{-1}$  with an intensity as high as 0.01 in absorbance units (or 0.022 in relative reflectivity units,  $\Delta R/R = 1 - I/I_0$ ) in CO-saturated 0.1 M HClO<sub>4</sub> electrolyte. This band was assigned to linearly bonded CO molecules, CO<sub>L</sub>, on Au. The bridge-bonded CO (CO<sub>B</sub>) is much weaker. The intensity of CO<sub>L</sub> is 1 order of magnitude more intense than that observed on bulk Au electrodes by IRAS. Shown in Figure 4 are typical SEIRA spectra of CO on metal-coated Au electrodes in CO-saturated 0.1 M HClO<sub>4</sub> obtained at ca. 0.3 V (vs RHE), where CO can stably exist on the surfaces of both Pt group metals and Au. The spectra are obviously different from those for CO on Au. The higher frequency bands at 2035–2076  $\text{cm}^{-1}$  correspond to CO<sub>L</sub>, while bands at 1820–1959  $\text{cm}^{-1}$  correspond to bridge-

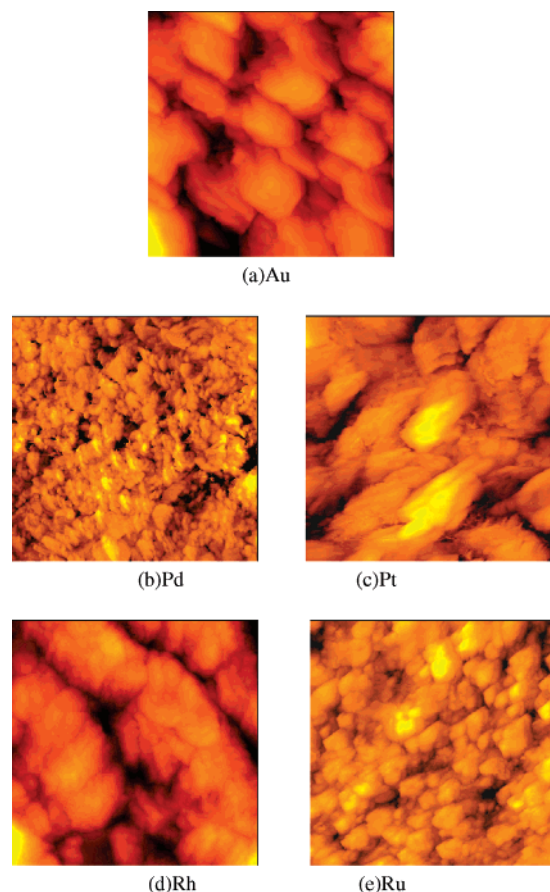


**Figure 3.** STM images (700 nm  $\times$  700 nm) of Au (a), Pd (b), Pt (c), Rh (d), and Ru (e) coated Au nanofilms.  $I_t = 5$  nA;  $V_b = 0.1$  V.

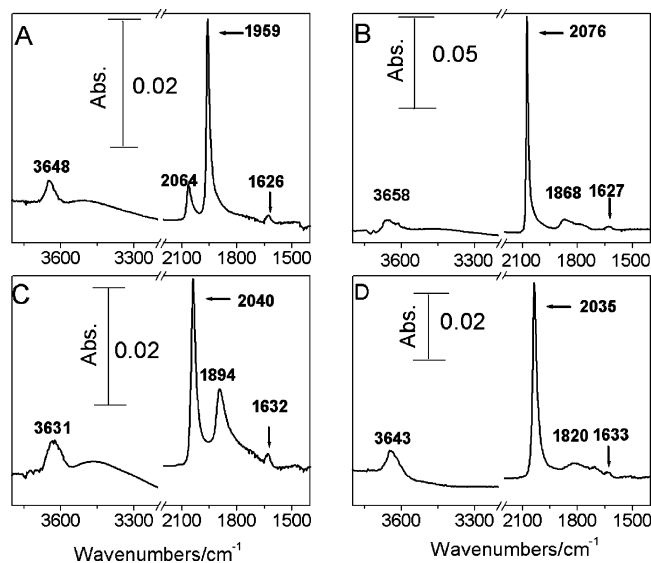


**Figure 4.** SEIRA spectra of CO on Pd (A), Pt (B), Rh (C), and Ru (D) nanofilm electrodes in 0.1 M HClO<sub>4</sub> saturated with CO at 0.3 V. Reference spectra were taken at 1.3 V in (A), 1.3 V in (B), 1.25 V in (C), and 1.0 V in (D), respectively.

bonded (CO<sub>B</sub>) or multicoordinated CO (CO<sub>M</sub>) adsorbed on the Pt group metals. No bands of CO adsorbed on Au are found. Assuming a detection sensitivity limit of  $2 \times 10^{-4}$  absorbance or  $5 \times 10^{-4}$  relative reflectivity of SEIRAS for CO<sub>L</sub> on chemically deposited Au electrodes,<sup>19,26</sup> at least 98% of Au sites are covered by the electrodeposited overlayers.

The CO bands shift to higher wavenumbers as the potential increases as has been reported on many bulk electrodes. The

**TABLE 1: Stark Tuning Rates of Major CO Bands for Electrodeposited Pd, Pt, Rh, and Ru Overlayers for Potentials Ranging from 0.1 to 0.6 V (RHE) in CO-Saturated 0.1 M HClO<sub>4</sub>**

| metal | major band      | Stark tuning rate (cm <sup>-1</sup> V <sup>-1</sup> ) |
|-------|-----------------|---|
| Pd    | CO <sub>B</sub> | ~37.4   |
| Pt    | CO <sub>L</sub> | ~30.0   |
| Rh    | CO <sub>L</sub> | ~34.5   |
| Ru    | CO <sub>L</sub> | ~45.0   |

rates of the potential-dependent peak shift, Stark tuning rates, for major CO bands are listed in Table 1. The frequency positions and relative intensities of CO<sub>L</sub> and CO<sub>B</sub> bands and the Stark tuning rates for the electrodeposited overlayers are in reasonable agreement with those for corresponding polycrystalline bulk electrodes.<sup>11,25</sup> These IR results as well as cyclic voltammograms clearly demonstrate that the Pt group metal overlayers are almost pinhole-free and have electrochemical and surface properties similar to those of the corresponding bulk metals.

Three other important features can be found from Figure 4. First, the peak intensities of major CO bands for the four metals (i.e., CO<sub>L</sub> bands for Pt, Rh, and Ru and CO<sub>B</sub> band for Pd) range from 0.03 to 0.11 in absorbance units, or  $\Delta R/R = 0.07$  to 22. According to Lamy and Beden,<sup>11</sup> the maximum theoretical band intensity for a CO adlayer on a smooth metal surface is around 0.003 in  $\Delta R/R$  units in the external reflection mode with unpolarized IR radiation. Hence the apparent surface enhancement factors of around 20–70 can be estimated for the Pt group metals from a simple comparison of peak intensities. The enhancement is the most significant for the electrodeposited Pt layer. The peak intensity of the CO<sub>L</sub> band (0.12 absorbance unit for unpolarized radiation) is twice that observed on a chemically deposited Pt nanofilm on Si (0.06 absorbance unit for unpolarized radiation and 0.3 absorbance unit for p-polarization).<sup>9</sup>

Second, the observed enhanced bands have unipolar band shapes similar to those observed on bulk metal surfaces. This is a marked difference from the enhanced bands observed on electrochemically deposited Pt group metal films on glassy carbon. The enhanced bands are inverted upside down and broadened on the latter films.<sup>15</sup> This significant advantage ensures an undisputed analysis and explanation for spectroscopic data obtained.

Third, the bands of water coadsorbed with CO molecules are clearly observed on all four metals investigated. The sharp bands at 3631–3658 cm<sup>-1</sup> can be assigned to  $\nu(\text{OH})$  and those at 1625–1633 cm<sup>-1</sup> to  $\delta(\text{HOH})$  of water molecules, the peak positions of which depend on the substrates and potentials.<sup>7,9a,12a,24</sup> The peak frequencies of the  $\nu(\text{OH})$  and  $\delta(\text{HOH})$  bands are remarkably higher and lower, respectively, compared with those of bulk water ( $\sim 3400$  and  $1645$  cm<sup>-1</sup>, respectively), indicating that the water molecules are free from hydrogen bonding. The bands of free water molecules have been already reported on Pt,<sup>9a</sup> Ru, and PtRu.<sup>12a</sup> According to the surface selection rule,<sup>2,12a</sup> the water is oriented on the surface with its C<sub>2</sub> axis perpendicular to the surface. Miki et al.<sup>9a</sup> ascribed these bands to water molecules embedded in the CO adlayer, while Watanabe et al.<sup>12a</sup> ascribed them to water molecules directly adsorbed on the surface. A further discussion on this issue will be given later.

**CO Oxidation on Pd.** The SEIRA-active nanofilms prepared by the two-step wet process are favorable for real-time monitoring and analysis of electrocatalytic reactions, as exemplified by the oxidative removal of a CO adlayer on the electrodeposited Pd overlayer. The upper panel of Figure 5 shows a series of

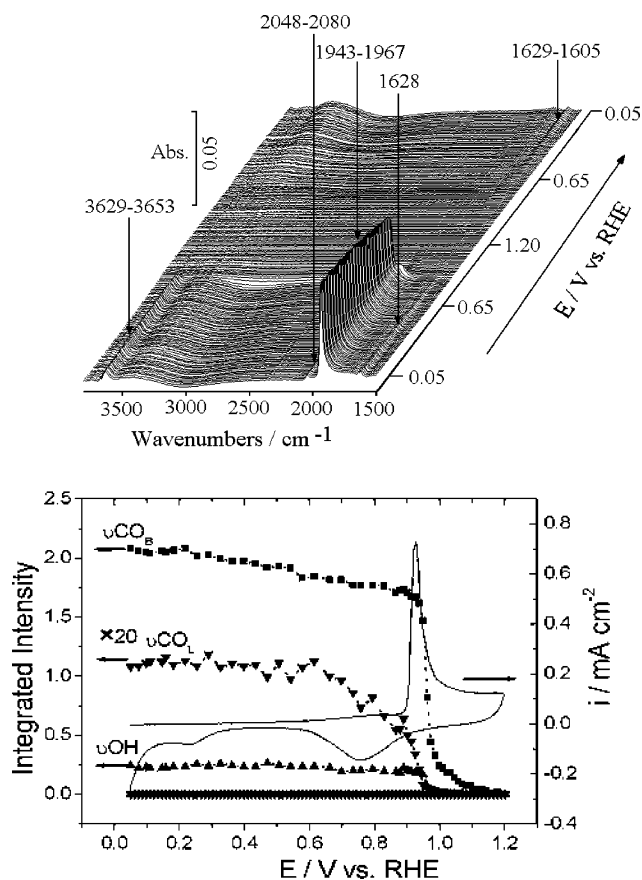


**Figure 5.** (upper) Series of time-resolved SEIRA spectra of CO-adsorbed Pd nanofilm electrode in 0.1 M HClO<sub>4</sub> collected sequentially during a potential sweep cycling 0.05 V → 1.2 V → 0.05 V at 50 mV s<sup>-1</sup>. The time resolution used and shown is 0.24 s. The Pd electrode was preadsorbed in CO-saturated 0.1 M HClO<sub>4</sub> solution at 0.05 V RHE for 15 min, and then the dissolved CO was purged with Ar bubbling for 30 min. (lower) Cyclic voltammogram recorded at 50 mV s<sup>-1</sup> during in situ ATR-SEIRAS measurement along with selected potential-dependent integrated intensities for IR bands of CO<sub>B</sub>, CO<sub>L</sub>, and coadsorbed H<sub>2</sub>O.

0.24 s time-resolved spectra of a Pd-coated Au electrode in 0.1 M HClO<sub>4</sub> (first saturated with CO and then dissolved CO was eliminated by Ar purging), which were collected sequentially during a potential sweep from 0.05 to 1.2 V and then back to 0.05 V at a scan rate of 50 mV s<sup>-1</sup>. The reference spectrum was taken at 1.2 V. The high sensitivity of ATR-SEIRAS enables the quick spectral acquisition with such a good signal-to-noise ratio. The lower panel of Figure 5 displays the plot of the normalized IR band intensities of CO<sub>L</sub>, CO<sub>B</sub>, and ν(OH) of the coadsorbed water against the potential together with the corresponding cyclic voltammogram. The sharp major CO oxidation peak locates at ca. 0.93 V in the voltammogram, with a broad oxidation prewave ranging from ca. 0.65 to 0.9 V. The minor CO<sub>L</sub> band decreases continuously at the potentials positive of 0.65 V, and disappears completely at ca. 0.95 V. The major CO<sub>B</sub> band and the free-water band decrease slightly in the oxidation prewave region, due probably to preferential oxidation of a fraction of weakly bound CO molecules at defect sites.<sup>27</sup> These two CO bands decrease sharply, responding to the rapid increase of the major CO oxidation current, together with the coadsorbed water band. It can also be seen that CO<sub>B</sub> can be removed at higher potentials in comparison to CO<sub>L</sub>. No conversion of CO<sub>L</sub> to CO<sub>B</sub> (or vice versa) was detected in the prewave region. These facts are in marked contrast with those reported on a Pt electrode, where CO<sub>B</sub> is more stable at relative

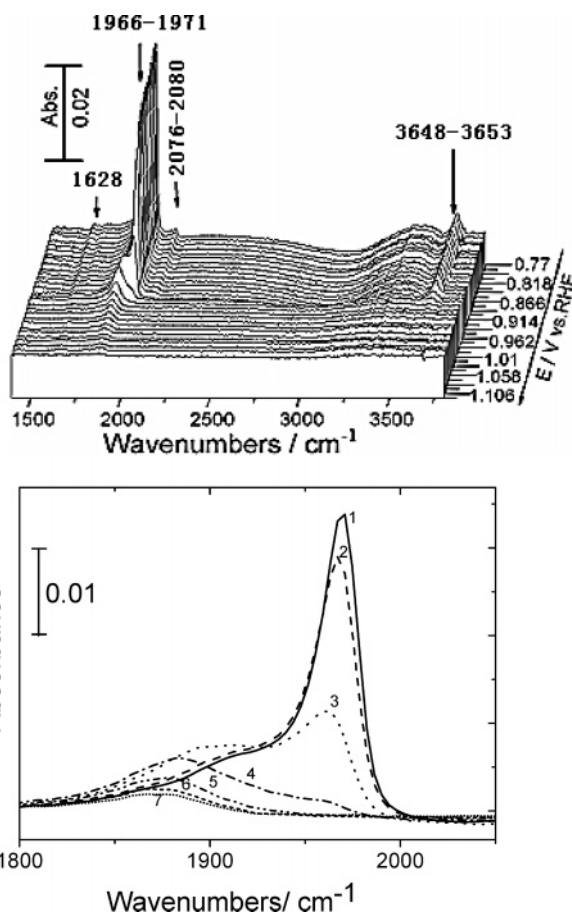


**Figure 6.** Zoomed three- (upper) and two-dimensional (lower) plots of potential-dependent SEIRA spectra for CO<sub>B</sub> band on Pd nanofilm electrode across the major CO oxidation peak in Figure 5. All the other conditions are the same as in Figure 5. For each labeled curve is given the median potential value at which the IR spectra were acquired during the forward potential sweep: curve 1, 0.926 V; curve 2, 0.938 V; curve 3, 0.950 V; curve 4, 0.962 V; curve 5, 0.974 V; curve 6, 0.986 V; and curve 7, 0.998 V.

lower potentials and CO<sub>B</sub> is converted to CO<sub>L</sub> with the increase of potential.<sup>27</sup> To see the CO oxidation process across the major current peak in more detail, selected spectra in the corresponding potential range in Figure 5 are replotted in Figure 6. It turned out that, as the oxidative removal of adsorbed CO<sub>B</sub> proceeds, the band at 1966 cm<sup>-1</sup> decreased and shifted to 1880–1900 cm<sup>-1</sup>, with the latter initially increasing and then decreasing in intensity as the potential moved positively, suggestive of the conversion of bridge to hollow bonding of CO species as its surface coverage turned lower.<sup>28</sup> It is stressed again that the high sensitivity of ATR-SEIRAS is indispensable for monitoring the irreversible conversion of adsorbed CO molecules occurring within 1 s.

The bands of free water molecules coadsorbed with CO mentioned above are observed also in Figures 5 and 6. The frequency of the relatively weak δ(HOH) band is virtually independent of potential scan, whereas that of the relatively strong ν(OH) band shifts linearly with potential from 3629 to 3653 cm<sup>-1</sup> at a rate of 25 cm<sup>-1</sup> V<sup>-1</sup> probably due to the Stark effect. These water bands completely disappeared in association with the oxidation of adsorbed CO, which may suggest an active involvement of coadsorbed water molecules in the oxidation of CO as an oxygen source.

It is worth noting that the sharp bands of free water molecules disappear after the oxidation of CO and never reappear. In the

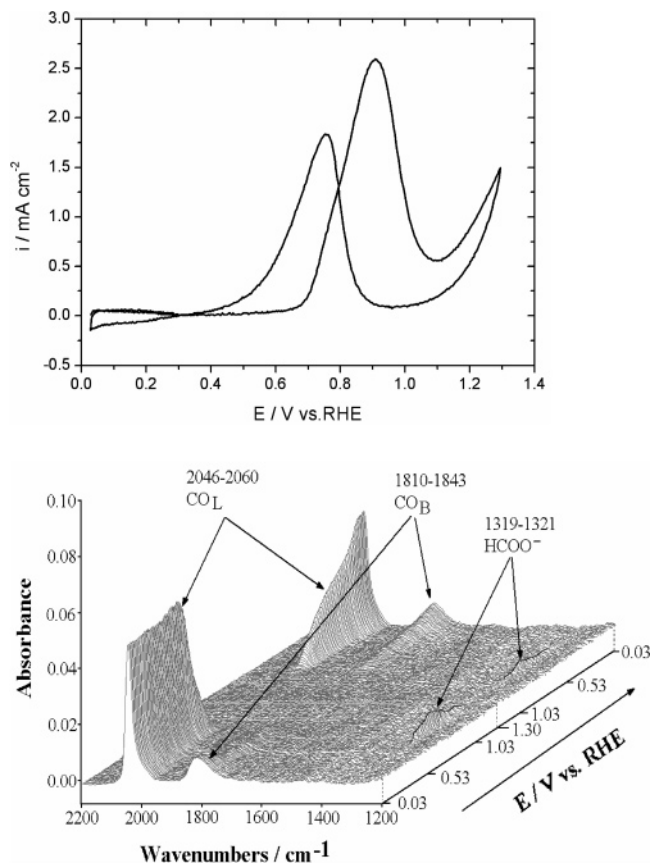


**Figure 7.** (upper) Cyclic voltammogram of Pt nanofilm electrode in 0.1 M HClO<sub>4</sub> + 0.5 M CH<sub>3</sub>OH during a potential sweep from 0.03 to 1.3 V and then back to 0.03 V (RHE) at a scan rate of 50 mV s<sup>-1</sup>. (lower) Series of corresponding time-resolved SEIRA spectra collected sequentially during the cyclic potential sweep. The time resolution used was 0.20 s. Reference spectrum was acquired at 1.3 V.

backward potential scan, a broad  $\nu(\text{OH})$  band and  $\delta(\text{HOH})$  band appear at  $\sim 3400$  and  $1605\text{--}1629\text{ cm}^{-1}$ , respectively, instead of the sharp bands after the Pd oxide layer was removed by reduction. The result clearly indicates that free water molecules can exist on the surface only when CO is adsorbed. Consequently, the sharp water bands can be ascribed more reasonably to those embedded in the CO adlayer<sup>9a</sup> than to those directly adsorbed on the surface,<sup>12a</sup> although the slight differences in peak positions on the four different metals seem to suggest some interactions between free water and the surfaces.

**Electrocatalytic Oxidation of Methanol on Pt.** The electrodeposited Pt nanofilm electrode has also been applied to an in situ study of the electrocatalytic oxidation of methanol. The time-resolved spectra of the Pt nanofilm electrode in 0.1 M HClO<sub>4</sub> + 0.5 M CH<sub>3</sub>OH obtained during cyclic voltammetric measurement are shown in Figure 7, which are exactly the same as for a chemically deposited Pt nanofilm on Si.<sup>9b</sup> Briefly, starting from the initial potential of 0.03 V, the intermediate for the self-dissociation of CH<sub>3</sub>OH on Pt at lower potentials is undoubtedly ascribed to adsorbed CO, as evidenced by the presence of CO<sub>L</sub> and CO<sub>B</sub> bands. As the methanol oxidation current starts to rise at ca. 0.7 V, a band at  $1320\text{ cm}^{-1}$  appears and is maximized around 1.0 V, suggestive of the adsorbed formate as the reactive intermediate species.<sup>9b</sup>

## Conclusion

We presented herein a ubiquitous two-step wet process, an economical and easy method to prepare nanofilms of Pt group

metals for electrochemical ATR-SEIRAS application. The strategy complements the one-step wet process for fabricating SEIRA-active surfaces which is currently limited to Au and Pt nanofilms on Si, and Ag and Cu nanofilms on Ge. With selected recipes and conditions for electrodeposition, Pt, Pd, Rh, and Ru overlayers with thicknesses ranging from several monolayers to tens of monolayers can uniformly coat onto a chemically deposited SEIRA-active Au nanofilm with almost no pinholes. The electrochemical behaviors of the Pt, Pd, Rh, and Ru electrodes were almost identical to those of bulk metals. In addition, these metal films exhibited extremely large SEIRA effects. The resultant SEIRA intensity of the probe molecule CO is 1 order of magnitude larger than the theoretical value calculated for CO adsorption at a smooth polycrystalline Pt electrode. For Pt electrodes prepared by the two-step method, the enhancement is a few times larger than those prepared by one-step wet process. Different from some earlier reports, the enhanced infrared spectra did not show any bipolar or inverted shapes, allowing for an easy and undisputed spectral analysis. The high detection limit of SEIRAS and the ATR configuration facilitated the simultaneous monitoring and analysis of molecular adsorption and reactions at these Pt group metals. As demonstrated, the two-step wet process is quite useful for in situ ATR-SEIRAS studies of electrochemical reactions. Efforts in further extension of metals are currently underway and will be reported in due course.

**Acknowledgment.** The NSFC (Nos. 20333040, 20473025), the SRFDP (No.20040246008), the NCET, and the SNPC (No. 0452nm064-2), China (W.-B.C.), and the MEXT (No. 14205121 and Priority Areas 417), Japan (M.O.), are gratefully acknowledged for financial support.

## References and Notes

- Hartstein, A.; Kirtley, J. R.; Tsang, J. C. *Phys. Rev. Lett.* **1980**, *45*, 201.
- (a) Osawa, M. In *Handbook of Vibrational Spectroscopy*; Chalmers J. M., Griffiths, P. R., Eds.; John Wiley & Sons: Chichester, UK, 2002; Vol. 1, pp 785–799. (b) Osawa, M. *Bull. Chem. Soc. Jpn.* **1997**, *70*, 2861.
- Kellner, R.; Mizaikoff, B.; Jakusch, M.; Wanzelbock, H. D.; Weissenbacher, N. *Appl. Spectrosc.* **1997**, *51*, 495.
- Sato, S.; Suzuki, T. *Appl. Spectrosc.* **1997**, *51*, 1170.
- (a) Cai, W.-B.; Wan, L.-J.; Noda, H.; Hibino, Y.; Ataka, K.; Osawa, M. *Langmuir* **1998**, *14*, 6992. (b) Cai, W.-B.; Amano, M.; Osawa, M. *J. Electroanal. Chem.* **2001**, *500*, 147.
- Maroun, F.; Ozanam, F.; Chazalviel, J. N.; Theiss, W. *Vib. Spectrosc.* **1999**, *19*, 193.
- Wandlowski, T.; Ataka, K.; Pronkin, S.; Dising, D. *Electrochim. Acta* **2004**, *49*, 1233.
- Bjerke, A. E.; Griffiths, P. R. *Appl. Spectrosc.* **2002**, *56*, 1275.
- (a) Miki, A.; Ye, S.; Osawa, M. *Chem. Commun.* **2003**, 1500. (b) Chen, Y. X.; Miki, A.; Ye, S.; Sakai, H.; Osawa, M. *J. Am. Chem. Soc.* **2003**, *125*, 3680. (c) Miki, A.; Ye, S.; Senzaki, T.; Osawa, M. *J. Electroanal. Chem.* **2004**, *563*, 23.
- Rodes, A.; Orts, J. M.; Pérez, J. M.; Feliu, J. M.; Aldaz, A. *Electrochim. Commun.* **2003**, *5*, 56.
- (a) Beden, B.; Lamy, C. In *Spectroelectrochemistry: Theory and Practice*; Gale, R. J., Ed.; Plenum Press: New York, 1988; Chapter 5. (b) Nichols, R. J. In *Adsorption of Molecules at Metal Electrodes*; Lipkowski, J., Ross, P. N., Eds.; VCH: New York, 1992; Chapter 7.
- (a) Yajima, T.; Uchida, H.; Watanabe, M. *J. Phys. Chem. B* **2004**, *108*, 2654. (b) Watanabe, M.; Zhu, Y. M.; Uchida, H. *J. Phys. Chem. B* **2000**, *104*, 1762. (c) Zhu, Y. M.; Uchida, H.; Watanabe, M. *Langmuir* **1999**, *15*, 875.
- Loster, M.; Friedrich, K. A. *Surf. Sci.* **2003**, *523*, 287.
- Bjerke, A. E.; Griffiths, P. R.; Theiss, W. *Anal. Chem.* **1999**, *71*, 1967.
- (a) Lu, G.-Q.; Sun, S.-G.; Cai, L.-R.; Chen, S.-P.; Tian, Z.-W.; Shiu, K.-K. *Langmuir* **2000**, *16*, 778. (b) Gong, H.; Sun, S.-G.; Li, J.-T.; Chen, Y.-J.; Lang, S.-P. *Electrochim. Acta* **2003**, *48*, 2933. (c) Sun, S.-G. In *Catalysis and Electrocatalysis at Nanoparticle Surfaces*; Wieckowski, A., Savinova, E. R., Vayenas, C. G., Eds.; Marcel Dekker: New York, 2003; Chapter 21.

- (16) Park, S.; Wiekowski, A.; Weaver, M. J. *J. Am. Chem. Soc.* **2003**, *125*, 2282.
- (17) (a) Pecharromán, C.; Cuesta, A.; Gutiérrez, C. *J. Electroanal. Chem.* **2002**, *529*, 145. (b) Ortiz, R.; Cuesta, A.; Marquez, O. P.; Marquez, J.; Mendez, J. A.; Cutierrez, C. *J. Electroanal. Chem.* **1999**, *465*, 234.
- (18) Miyake, H.; Osawa, M. *Chem. Lett.* **2004**, *33*, 278.
- (19) Miyake, H.; Ye, S.; Osawa, M. *Electrochem. Commun.* **2002**, *4*, 973.
- (20) (a) Zou, S.; Weaver, M. J. *Anal. Chem.* **1998**, *70*, 2387. (b) Zou, S.; Williams, C. T.; Chen, E. K.-Y.; Weaver, M. J. *J. Am. Chem. Soc.* **1998**, *120*, 3811.
- (21) (a) Cai, W. B.; Ren, B.; Liu, F. M.; Li, X. Q.; She, C. X.; Cai, X. W.; Tian, Z. Q. *Surf. Sci.* **1998**, *406*, 9. (b) Tian, Z. Q.; Ren, B.; Wu, D. Y. *J. Phys. Chem. B* **2002**, *106*, 9463. (c) Gomez, R.; Perez, J. M.; Solla-Gullon, J.; Montiel, V.; Aldaz, A. *J. Phys. Chem. B* **2004**, *108*, 9943.
- (22) Kern, W.; Puotinen, D. A. *RCA Rev.* **1970**, *31*, 187.
- (23) Strbac, S.; Maroun, F.; Magnussen, O. M.; Behm, R. J. *J. Electroanal. Chem.* **2001**, *500*, 479.
- (24) (a) Ataka, K.; Yotsuyanagi, T.; Osawa, M. *J. Phys. Chem.* **1996**, *100*, 10664. (b) Ataka, K.; Osawa, M. *Langmuir* **1998**, *14*, 951.
- (25) Gutierrez, C.; Caram, J. A.; Beden, B. *J. Electroanal. Chem.* **1991**, *305*, 289.
- (26) Sun, S.-G.; Cai, W.-B.; Wan, L.-J.; Osawa, M. *J. Phys. Chem. B* **1999**, *103*, 2460.
- (27) (a) Lebedeva, N. P.; Koper, M. T. M.; Feliu, J. M.; van Santen, R. A. *J. Electroanal. Chem.* **2002**, *524*, 242. (b) Markovic, N. M.; Schmidt, T. J.; Grgur, B. N.; Gasteiger, H. A.; Behm, R. J.; Ross, P. N. *J. Phys. Chem. B* **1999**, *103*, 8568.
- (28) Zou, S.; Gomez, R.; Weaver, M. J. *J. Electroanal. Chem.* **1999**, *474*, 155.